



## Effect of processing conditions and material attributes on the design space of lysozyme pellets prepared by extrusion/spheronization

Yousif H-E.Y. Ibrahim<sup>a</sup>, Patience Wobuoma<sup>a</sup>, Katalin Kristó<sup>a</sup>, Ferenc Lajkó<sup>b</sup>, Gábor Klivényi<sup>b</sup>, Béla Jancsik<sup>c</sup>, Géza Regdon jr<sup>a</sup>, Klára Pintye-Hódi<sup>a</sup>, Tamás Sovány<sup>a,\*</sup>

<sup>a</sup> University of Szeged, Institute of Pharmaceutical Technology and Regulatory Affairs, Eötvös U. 6., H-6720, Szeged, Hungary

<sup>b</sup> Opulus Ltd, Fűrj Utca 92/B, H-6726 Szeged, Hungary

<sup>c</sup> Opulus Ltd, 1951 NW 7th. Avenue, 33136, Miami, FL, USA

### ARTICLE INFO

#### Keywords:

Lysozyme  
Polyol  
Extrusion/spheronization  
Quality by design  
Design space  
Material attributes

### ABSTRACT

The present work aimed to investigate the impact of the critical material attributes on the design space of the production of lysozyme pellets with suitable biological and physical properties for the subsequent coating process. The effect of two brands of both lysozyme and conformation stabilizing mannitol on the behavior of the composition in an extrusion/spheronization process was studied, while the experiments were designed according to 2<sup>3</sup> factorial design. The kneading of the mass was carried out in a high shear granulator equipped with a specially designed granulation chamber (Opulus Ltd, Hungary) constructed with seven built-in sensors for the measurement of temperature and relative humidity (RH). The special chamber is a novel tool for the identification of the critical points during processing a thermolabile drug by providing the online monitoring of critical environmental parameters and could be used to accurately determine the effect of critical process parameters and material attributes. The prepared samples were investigated for their biological and physical properties. It was found that the critical material attributes have a potential effect on the production process and product quality, and highly influence the size of the process design space. Therefore, the screening of the formulation materials is a key factor in macromolecular drug development.

### 1. Introduction

Flourishing in the biotechnological field has produced numerous macromolecules, such as proteins and peptides, which play a great role in managing and treating various diseases, e.g. autoimmune, neurodegenerative and cancer diseases [1]. Their oral delivery remains an attractive alternative to invasive routes because it offers cost-effectiveness as well as patient convenience and compliance [2,3]. To date, they are administered parenterally due to their low bioavailability from other alternative routes of administration, including the oral route [4]. Egg-white lysozyme occurs in many vertebrates and insects, and this diversity of the source renders it the most affordable enzyme [5]. It is harmless to human cells and effectively lyses or inhibits the growth of several pathogens responsible for food spoilage and food-borne diseases; therefore it has a substantial role as a preservative in the food industry [6]. Lysozyme is commonly known as an antimicrobial agent mainly against Gram-positive bacteria and some fungi. Bactericidal activity was due to an approved membrane disturbing effect

on the peptidoglycan layers of the bacterial cell wall [7–9]. Due to presence of an outer membrane consisting of lipopolysaccharide, lysozyme is ineffective against Gram-negative bacteria, and consequently various methods are available to expand the activity, such as conjugation and combination with a permeation enhancing agent [10]. Therefore, its successful formulation in a stable oral solid dosage form may contribute to managing and controlling many diseases caused as a result of food contamination.

Compared to single unit solid dosages, multiparticulate dosages, for example pellets, are acquiring definite priority for many reasons, such as anticipated gastric emptying time, reduced riskiness of dose dumping, spherical shape and hence easiness to coat, adjustable release designs, as well as even and predictable distribution through the gastrointestinal tract (GIT), resulting in enhanced drug dissolution, which leads to increased bioavailability with low inter- and intra-subject variations [11–13]. Accordingly, multiparticulates are the most suitable for the development of an orally ingested solid dosage form to deliver a macromolecular drug.

\* Corresponding author.

E-mail address: [sovanytamás@gmail.com](mailto:sovanytamás@gmail.com) (T. Sovány).

<https://doi.org/10.1016/j.jddst.2021.102714>

Received 10 February 2021; Received in revised form 4 June 2021; Accepted 6 July 2021

Available online 21 July 2021

1773-2247/© 2021 The Authors.

Published by Elsevier B.V. This is an open access article under the CC BY-NC-ND license

(<http://creativecommons.org/licenses/by-nc-nd/4.0/>).

The pelletization process is an agglomeration procedure that converts the homogenized powders of a drug and excipients into relatively high density, free-flowing spherical or semi-spherical units of narrow size distribution called pellets, with a dimension of 500–1500  $\mu\text{m}$  [14–16]. Among the pellet production methods, the extrusion and spheronization method is used frequently and is widely considered as a potential future method, due to its ability to produce more dense spheres with higher drug-loading capacity while retaining their small size, and thus the process is considered more efficient than other pelletization methods [17–19]. For pellets to be layered or coated, roundness [20] and aspect ratio [21] are the most investigated parameters to evaluate the suitability of pellets for sub-coating/coating processes as well as for estimating flowability. However, in the case of a macromolecular drug such as lysozyme, the mechanical and thermal stresses encountered during processing into an effective dosage form should be carefully evaluated [22] since these stresses might have a reverse effect on enzyme activity when the moisture content is high, especially during high shear pelletization [23]. Accordingly, the implementation of a specially instrumented chamber for the analysis of temperature and relative humidity and the design of experiment as tools of quality by design could be vital to assessing the risk factors encountered during the pelletization process and represent helpful tools for understanding the effect of different process parameters and material characteristics on the quality of the produced pellets.

Similarly, polyols such as glycerol, propylene glycol, trehalose and mannitol can be used to stabilize lysozyme conformation through their exclusion from the vicinity of macromolecules, and thus the interaction with proteins is unfavourable. Among them, mannitol was found to stabilize lysozyme mainly against aggregation [24,25]. Therefore, mannitol can be used to preserve the lysozyme conformation by preventing the misfolding of the enzyme, and hence the activity during the various processing steps of pelletization might be maintained.

The present study is the continuation of a previous experiment series [1,22], aimed at developing a multiparticulate system for lysozyme delivery. The aim of the present phase of the study is to investigate the

impact of the material attributes on the process design space, and furthermore to clarify the impact of mechanical and thermal stress encountered during the various production steps on the enzyme activity of the prepared pellets.

## 2. Materials and methods

### 2.1. Materials

Two brands of Egg-white lysozyme (Mw: 14.3 kDa), with different stabilities Lysoch-40000 (Handary SA, Brussels, Belgium) here referred to as “Lyso-1” and a CAT. HY-B2237/CS-7671 (MedChemExpress, Hungary), referred to as “Lyso-2” were used as model proteins. The scanning electron micrographs (Fig. 1a and b) showed no considerable differences in the size or morphology of Lyso-1 and Lyso-2, but there are considerable differences between their stability, since Lyso-1 may be stored under ambient conditions up to 24 month, while Lyso-2 should be stored at  $-20\text{ }^{\circ}\text{C}$ . According to our hypothesis, the poorer thermal stability may negatively affect enzymatic activity, but with careful design, it is still possible to produce pellets of the required quality. Conventional crystalline (Hungaropharma Ltd., Budapest, Hungary) and directly compressible spray-dried (Pearlitol SD-200, Roquette Pharma, France) mannitol (referred to as CM and SDM, respectively) served as conformation stabilizers. The CM have big columnar/tabular crystals with sharp edges, and wide particle size distribution (Fig. 1c), while SDM have spherical particles with more narrower size distribution (Fig. 1d), which may be considered as aggregates of columnar microcrystals. Further difference that while CM is pure  $\beta$  form, SDM is a mixture of  $\alpha$  and  $\beta$  forms, which exerted smaller elasticity in compression studies. Microcrystalline cellulose (Avicel pH 101, FMC Biopolymer, Philadelphia, USA; Mw: approx. 160 kDa) referred to as MCC, was utilized as pellet former and drug carrier, lyophilized *Micrococcus lysodeikticus* (Sigma-Aldrich, USA) was used as standard reagent for lysozyme activity investigation.

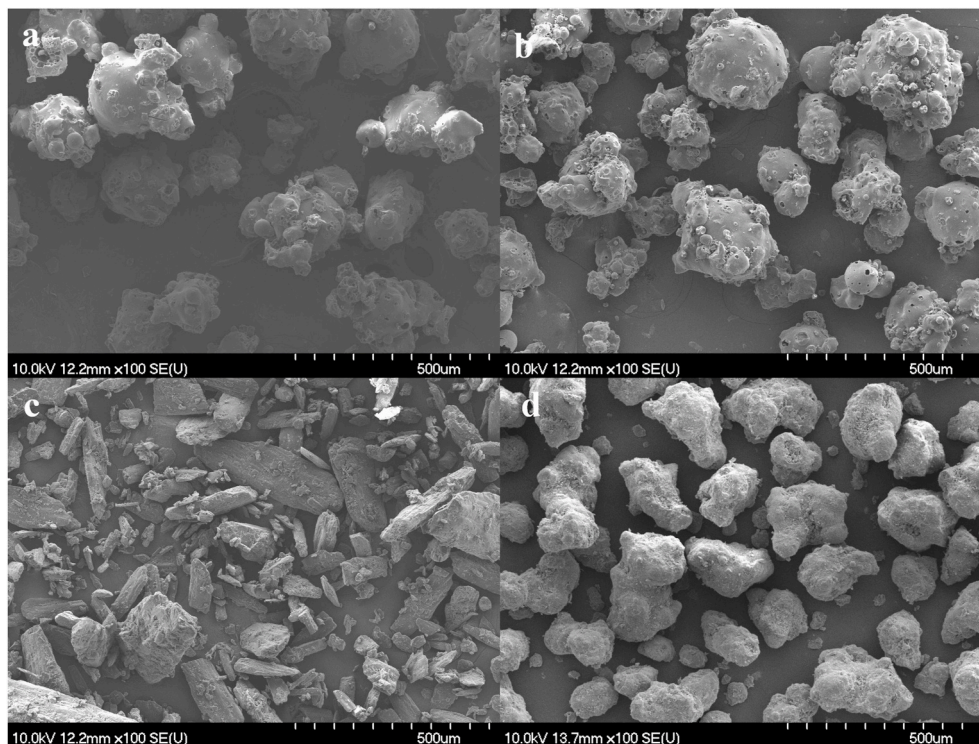


Fig. 1. Scanning electron micrographs of lyso-1 (a), lyso-2 (b), CM (c) and SDM (d).

## 2.2. Methods

### 2.2.1. Design of experiments

The experimental design was made according to  $2^3$  full factorial design with one central point. The impeller speed ( $x_1$ ), liquid addition rate ( $x_2$ ) and extrusion speed ( $x_3$ ) were studied as independent factors, while the optimization parameters were: enzyme activity ( $y_1$ ), pellet hardness ( $y_2$ ), moisture content ( $y_3$ ), roundness ( $y_4$ ) and aspect ratio ( $y_5$ ). The effect of factors and factor interactions on the optimization parameters was evaluated statistically by using Statistica v. 13.5. software (Tibco Statistica Inc, Palo Alto, CA, USA).

### 2.2.2. Homogenization

100 g of powder mixtures composed of Lyso-1 or Lyso-2, CM or SDM and MCC in a ratio of 1:4:5, respectively, were homogenized in a Turbula mixer (Willy A. Bachofen Maschinenfabrik, Basel, Switzerland) for 10 min. The composition of the homogenized powder mixtures is shown in Table 1.

### 2.2.3. Estimation of water quantity

The amount of the granulating liquid used to produce a moisturized plastic mass of a powder mixture to be ideal for extrusion/spheronization is critical, since the liquid quantity will affect the quality of the extrudate, as well as the hardness and the sphericity of the particles [26, 27]. Therefore, the water quantity required for wet granulation was estimated by determining the Enslin number, which is a simple measurement and equals the quantity of water absorbed by 1 g of the powder mixture (ml/g). The equipment is simple and consists of a G4 glass filter and a pipette with 0.01 accuracy. 0.5 g of each homogenized powder mixture was dispersed as a monolayer over a filter paper which was placed horizontally at the bottom of the glass filter, and the maximum water uptake was determined. The experiment was performed three times.

### 2.2.4. Wet granulation

The homogenized mixtures of the powder samples were wetted and kneaded in a ProCepT 4M8 high shear granulator (ProCepT nv, Zelzate, Belgium) at different impeller speeds ( $x_1$ ) and liquid addition rates ( $x_2$ ). The impeller and chopper were located vertically; the processing parameters are illustrated in Table 2 below. 60 ml of purified water was added at different rates (-1, 0 and + 1 level), followed by 60 s wet massing time. Wet granulation and kneading were performed in a specially designed Teflon granulation chamber (Opulus Ltd., Szeged, Hungary) equipped with three immersed PyroDiff® sensors (channel 1, 2 and 3) located at different heights from the bottom of the chamber and at different distances from the chamber wall, as demonstrated in Fig. 2. They were connected directly to a computer via an interface, and four calibrated PyroButton-TH® sensors (ISO 17025) were equipped on the chamber wall at different positions (at the bottom, 42 mm, 65 mm and 87 mm from the bottom). The sensors were programmed to continuously measure the change in temperature and relative humidity (RH) in every 2 s during the granulation, at a temperature and humidity resolution of 0.0626 °C and 0.04 % RH, respectively. In addition, the infrared temperature sensor of the high shear granulator was set to continuously measure the temperature during granulation. The kneaded wet mixtures were preserved in tightly closed containers until extrusion/

spheronization.

### 2.2.5. Extrusion and spheronization

The kneaded wet masses were extruded with a single-screw extruder (Caleva Process Solutions Ltd., Sturminster Newton, UK), equipped with an axial screen of 4-mm thickness and having 16 dies with a diameter of 1 mm. The extruder was equipped with a laboratory-developed water-cooling jacket to maintain the temperature constant during extrusion. Extrusion was performed at different extrusion rates ( $x_3$ ) (70, 95 and 120 rpm) and at a constant feeding rate of 5 g/min. The obtained extrudates were preserved in moisture-retentive containers to prevent water loss.

The extruded samples were spheronized with a Caleva MBS spheronizer (Caleva Process Solutions Ltd., Sturminster Newton, UK). 17 g of each extruded sample was spheronized at a speed of 2000 rpm for 1 min (according to the preformulation study). The obtained pellets were dried for 24 h under ambient conditions ( $22 \text{ °C} \pm 1$ ,  $31 \pm 2\%$  RH).

### 2.2.6. Pellet activity investigation

The biological activity ( $y_1$ ) of the prepared pellets was measured via the degradation of lyophilized *Micrococcus lysodeikticus* by using a Genesys 10 S UV-VIS Spectrometer (ThermoScientific, Waltham, MA, USA). 70 mg of lyophilized bacteria was suspended in 100 ml of phosphate buffer (pH 6.24), the base absorption at 450 nm was around 0.7. The absorption of the bacterial suspension was measured for 5 min before each test to reduce the error arising from bacterial sedimentation. 100 mg of pellet or 10 mg of crude lysozyme were dissolved in 25 ml of phosphate buffer. 0.1 ml of pellet/or crude lysozyme solution was added to 2.5 ml of bacterial suspension and shaken for 20 s in a quartz cuvette, then the change in bacterial absorption was measured for 5 min. Pellet activity was calculated from the percentage degradation of the bacterial cells relative to crude lysozyme activity as a reference.

### 2.2.7. Hardness and deformation

Deformation force ( $y_2$ ) and behavior were investigated with a custom-made texture analyzer; the equipment and its software were developed at the University of Szeged, Institute of Pharmaceutical Technology and Regulatory Affairs. The equipment consists of a sample holder at the base and a probe moving vertically at a speed of 20 mm/min. The test was conducted in the force range of 0–50 N. The deformation characteristics and breakage force of pellets ( $n = 20$  for each sample) were obtained and the average and SD were calculated.

### 2.2.8. Moisture content

The moisture content ( $y_3$ ) of the prepared pellets was measured by using a Mettler-Toledo HR73 (Mettler-Toledo Hungary Ltd., Budapest, Hungary) halogen moisture analyzer. The moisture content of approximately 0.5 g of each sample was measured in triplicate at the drying temperature of 105 °C until a constant weight was obtained.

### 2.2.9. Size and shape study

The size and shape ( $y_4$  and  $y_5$ ) of the prepared samples were investigated by using a system consisting of a stereomicroscope and a ring light with a cold light source (Carl Zeiss, Oberkochen, Germany). The images were analyzed with Leica Qantimet 500 C image analysis software (Leica Microsystems, Wetzlar, Germany), and the area, length, breadth, perimeter, convex perimeter, roundness and aspect ratio of 100 pellets were measured or calculated. The roundness and aspect ratio are the most common shape parameters used to characterize the shape of pellets and are calculated by the applied Leica Q500MC software using the following equations:

$$\text{Roundness} = \frac{\text{Perimeter}^2}{4 * \pi * \text{Area} * 1.064} \quad (1)$$

$$\text{Aspect ratio} = \frac{d_{\text{max}}}{d_{\text{min}}} \quad (2)$$

**Table 1**  
Composition of prepared powder mixtures.

Excipients	C1 (g)	C2 (g)	C3 (g)
Lyso-1	10	10	–
Lyso-2	–	–	10
CM	40	–	40
SDM	–	40	–
MCC	50	50	50

**Table 2**  
Processing parameters of kneading, extrusion and spherization.

Kneading	Process-1		Process-2		Process-3		Process-4		Process-5
Impeller speed (rpm) ( $x_1$ )	500 (-1)		500 (-1)		1500 (+1)		1500 (+1)		1000 (0)
Liquid addition rate (ml/min) ( $x_2$ )	5 (-1)		10 (+1)		5 (-1)		10 (+1)		7.5 (0)
Purified H <sub>2</sub> O (ml)	60		60		60		60		60
Chopper speed (rpm)	500		500		500		500		500
<b>Extra./spheron.</b>									
Extrusion speed ( $x_3$ )	70 (-1)	120 (+1)	70 (-1)	120 (+1)	70 (-1)	120 (+1)	70 (-1)	120 (+1)	95 (0)
Spher. speed (rpm)	2000	2000	2000	2000	2000	2000	2000	2000	2000
Spher. time (min)	1	1	1	1	1	1	1	1	1
Spher. amount (g)	17	17	17	17	17	17	17	17	17
Sample code	LysC <sup>a</sup> -11	LysC-12	LysC-21	LysC-22	LysC-31	LysC-32	LysC-41	LysC-42	LysC-c

<sup>a</sup> C: referring to the composition; 1, 2 and 3 for the first (C1), second (C2) and third (C3) composition, respectively.

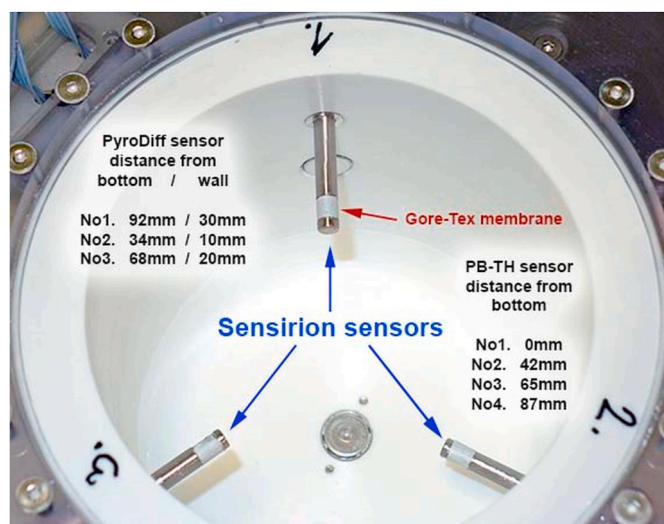


**Fig. 2.** Kneading chamber showing the configuration of immersed (PyroDiff®) and PyroButton-TH® sensors.

where *Perimeter* is the total length of boundary of the feature, *Area* is calculated from the total number of detected pixels within the feature, while  $d_{max}$  and  $d_{min}$  are the longest and shortest Feret diameter measured.

### 2.2.10. Scanning electron microscopy

The morphology and size of the raw materials were investigated by Scanning Electron Microscope (SEM) (Hitachi 4700, Hitachi Ltd., Tokyo, Japan). The samples were coated with a conductive gold thin layer by a sputter coating unit (Polaron E5100, VG Microtech, UK), images were taken at an accelerating voltage of 10.0 kV, the used air pressure was 1.3–13 mPa during the analyses. The particle size was determined using Image J 1.47 t (National Institute of Health, Bethesda, MD, USA) software.

## 3. Results and discussion

### 3.1. Investigation of the change in temperature and RH% during the kneading phase

In our previous studies [1,22] an unexpected effect of the applied kneading parameters was observed on the enzyme activity of the prepared pellets. One of the key objectives of the present study was to clarify the reason for this effect via the use of a special kneading chamber, which enabled the determination of the variations of temperature and relative humidity at representative points of the chamber. In order to reveal if the chamber wall (Teflon) has any effect on the behavior of the materials, we repeated the previous experiments

obtained in a glass chamber with the same quality of materials (composition C1).

The variation of the recorded values was attributed to the sensor location and its distance from the impeller rotation axis, as illustrated above (Fig. 2), and the detected local temperatures may be considerably higher than the general temperature recorded by the granulator's own built-in sensor [23]. The variation of temperature and humidity with the various experimental settings can be found in the supplementary material.

As expected, at a lower (-1) level of impeller speed, the internal chamber temperature was relatively low and constant throughout the wet kneading period, which is advantageous for processing thermolabile molecules. Under these conditions, the liquid addition rate has less impact on the temperature value, as demonstrated in Fig. 3, where the difference between the starting and final temperatures is displayed throughout the various experimental settings.

When operating at a higher (+1) level of impeller speed (process 3 and 4), the liquid addition rate exhibited more considerable influence on the temperature distribution inside the chamber, although it was only partially able to compensate for the temperature increase which was induced by mechanical friction between the kneaded mass, impeller, and chamber wall. Overall, the temperature change mostly depends on impeller speed, and it exhibited a linear relation with the investigated parameters (Eq. (3)).

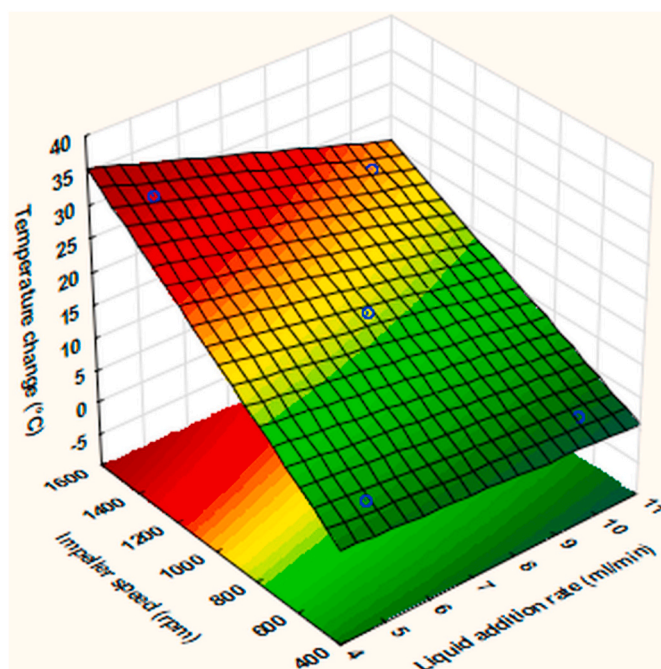


**Fig. 3.** Temperature change in the kneading phase.

$$y_{\Delta T} = 15.409 + \mathbf{10.643}_{x_1} - 3.176_{x_2} - 1.633_{x_1x_2} \quad (3)$$

$$R^2 = 0.99836 \text{ Adj } R^2 = 0.99344 \text{ MS Residual} = 0.828245$$

In contrast, the variation of system relative humidity did not follow the expectations since the increasing liquid addition rate resulted in a reduced increment of relative humidity. This unexpected phenomenon may be due to the insufficient equilibration time of the moisture content on the solid-air interface. The highest increment in the system RH% values was recorded in the central point (Fig. 4). The low adj.  $R^2$  and high curvature coefficient of the corresponding Equation (4), indicates poor model quality, which may be due to a strong nonlinear relationships between the tested factors and RH%.

$$y_{RH\%} = 53.6158 - 2.3742_{x_1} - 2.2925_{x_2} \quad (4)$$

$$R^2 = 0.80017 \text{ Adj } R^2 = 0.20067 \text{ MS Residual} = 31.4534 \text{ Curvature} = 10.148$$

The increasing impeller speed also decreases the general increment in the system RH%, which may indicate that more intensive mixing promotes the uniform distribution of moisture, which increases the amount of the surface adsorbed fraction. Nevertheless, at a lower impeller speed, RH% was comparable in the whole granulation chamber, but increasing impeller speed resulted in greater RH% variation with a rapid increase in RH% values throughout the granulation chamber (Figs. S3 and S4 in the supplementary material). This may be due to the increased evaporation rate in the regions with elevated temperature, which is supported by the similar distribution of temperature and RH% values (Figs. S1 and S3 in the supplementary material).

The results confirmed our original hypothesis that there are differences in the distribution of temperature and relative humidity inside the granulation chamber, which may result in the formation of hot spots, which represent the critically degrading microenvironment for sensitive drugs. Nevertheless, it should be noted that despite the similar tendencies, generally better enzyme activities (See chapter 3.2) were recorded than previously in the glass chamber (92.67 % vs. 58.98 % (5) of enzyme activity). This phenomenon may be explained by the different thermal conductivity of Teflon and glass (0.25 W/mK vs. 0.96–1.05 W/mK), which will result in less localized thermal elevation and therefore the formation of bigger hot spots in the glass chamber.

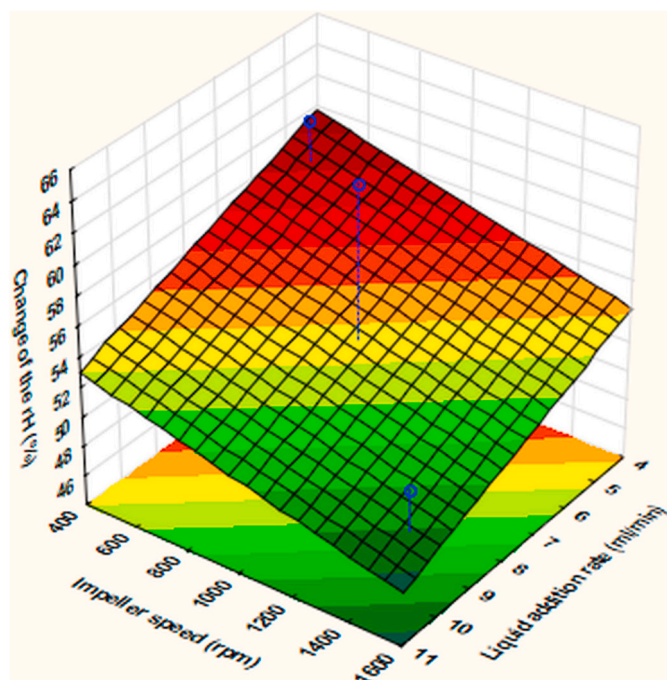


Fig. 4. Relative humidity change in the kneading phase.

### 3.2. Investigation of the impact of material attributes on pellet quality

Despite the considerable variation in temperature and humidity distribution, the detected maximum temperatures (Fig. 5) are good indicators of material behavior during the kneading phase.

It is clearly visible that at low shear rates (process 1 and 2) there is no difference in the recorded temperature. In contrast, at high levels of impeller speed and low levels of liquid addition, C2 exhibited considerably lower maximum temperature compared to C1 and C3. Schaefer and Mathiesen and Kristó et al. reported that the increase in temperature in high shear granulation is mainly attributed to the conversion of mechanical energy input into heat of friction within the moist mass [23, 28]. Therefore, the lower temperature elevation upon high mechanical attrition may be due to the better deformation properties of SDM over CM.

The temperature excess arising in the case of C1 may be compensated for by the cooling effect of an increased liquid addition rate while it is related only to the presence of CM. However, if CM is combined with lyso-2 in C3, the further increasing friction results in a much higher temperature than a composite containing SD lyso-1 (C1 and C2), despite the increased liquid addition rate. In conclusion, in spite of the general physicochemical similarities and similar liquid uptake pattern (0.6 ml/g) of the SD and C form of raw materials, the material attributes showed obvious differences in thermal behavior upon the applied mechanical stress, especially at higher shear rates. This finding is supported by Hulse et al., who reported that despite the similarity in the thermal behavior of CM and its different forms such as SDM, a full characterization is required as a preformulation step because these polymorphs are dissimilar in their physical properties [29]. Overall, the method of raw material production (i.e. conventional crystallization, or spray drying) has an effect on the thermomechanical response upon exposure to higher mechanical stress and may considerably influence the critical quality attributes of the final product (Tables 3–5).

#### 3.2.1. Biological activity

For a macromolecular drug (such as lysozyme) to be formulated into multiparticulates, biological activity is the most important criterion that should be retained for the finished product, particularly when manufacturing processes operate at high shear rates, usually accompanied with an elevation of temperature and high attrition. Accordingly, biological activity might be diminished as a result of protein folding or denaturation.

The statistically obtained equations describing the relationship between factors  $x_1$ ,  $x_2$  and  $x_3$ , and the optimization parameter ( $y_1$ ) are listed below. The statistically significant factor coefficients are shown in bold. The second subscript number of the optimization parameters ( $y$ ) refers to the composition (C1, C2 or C3). The coefficients of the factors (variables) and their interactions show the changes in the optimization parameters when the value of the variable increased from 0 to +1 level. In order to get a good fit by increasing the  $adjR^2$  values, some unnecessary elements have been omitted from the equations.

$$y_{11} = 92.267 - 0.597_{x_1} + 3.314_{x_2} - 4.926_{x_3} + 3.749_{x_1x_2} - 5.550_{x_1x_3} - 2.786_{x_1x_2x_3} \quad (5)$$

$$R^2_{adj} = 0.9814 \text{ MS Residual} = 1.667 \text{ Curv. coeff.} = -3.282$$

$$y_{12} = 96.56 + \mathbf{4.00}_{x_1} + \mathbf{1.51}_{x_2} - \mathbf{1.89}_{x_1x_2} - \mathbf{3.00}_{x_1x_3} + \mathbf{4.78}_{x_2x_3} + \mathbf{1.18}_{x_1x_2x_3} \quad (6)$$

$$R^2_{adj} = 0.9995 \text{ MS Residual} = 0.0369 \text{ Curv. coeff.} = -12.41$$

$$y_{13} = 81.45 - 4.50_{x_1} + 1.37_{x_2} + 2.75_{x_3} - 1.49_{x_1x_2} - 1.29_{x_1x_3} + 0.46_{x_1x_2x_3} \quad (7)$$

$$R^2_{adj} = 0.9771 \text{ MS Residual} = 1.3337 \text{ Curv. coeff.} = -14.78$$

The average enzyme activity was relatively high (92.267 % and 96.56%) for C1 and C2 (Eqs. (5) and (6), respectively). However, while there were no statistically significant coefficients for C1, for C2 the

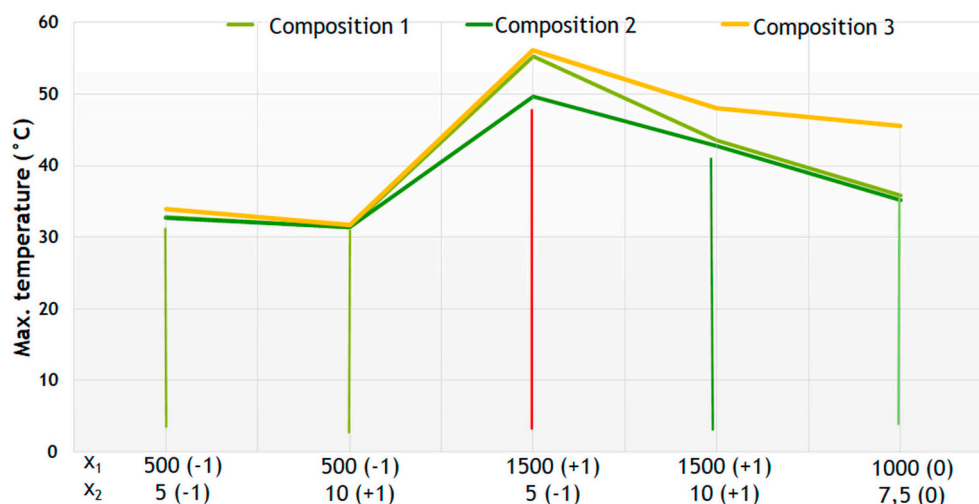


Fig. 5. Maximum recorded temperature under different processing conditions for the various compositions (C1, C2 and C3).

Table 3

Physical properties and biological activity of C-1-pellets.

Sample	Activity% ( $y_{11}$ )	Hardness (N) ( $y_{21}$ )	MC% ( $y_{31}$ )	Roundness ( $y_{41}$ )	Aspect ratio ( $y_{51}$ )
Lys1-11	95.92	15.55 ± 1.67	0.93 ± 0.02	1.13 ± 0.13	1.14 ± 0.10
Lys1-12	92.75	13.03 ± 1.10	0.51 ± 0.03	1.11 ± 0.08	1.13 ± 0.06
Lys1-21	88.56	13.00 ± 1.17	0.62 ± 0.02	1.17 ± 0.10	1.18 ± 0.10
Lys1-22	111.56	11.60 ± 1.24	0.44 ± 0.01	1.15 ± 0.10	1.16 ± 0.10
Lys1-31	90.68	14.64 ± 1.54	0.59 ± 0.02	1.15 ± 0.07	1.16 ± 0.07
Lys1-32	76.46	12.50 ± 1.55	0.41 ± 0.03	1.14 ± 0.07	1.15 ± 0.06
Lys1-41	96.30	14.00 ± 1.05	0.63 ± 0.02	1.14 ± 0.09	1.14 ± 0.06
Lys1-42	85.93	13.60 ± 1.41	0.40 ± 0.01	1.15 ± 0.12	1.14 ± 0.07
Lys1-C	88.99	14.04 ± 1.05	0.77 ± 0.02	1.13 ± 0.10	1.13 ± 0.05

Table 4

Physical properties and biological activity of C-2 -pellets.

Sample	Activity% ( $y_{12}$ )	Hardness (N) ( $y_{22}$ )	MC% ( $y_{32}$ )	Roundness ( $y_{42}$ )	Aspect ratio ( $y_{52}$ )
Lys2-11	89.84	13.01 ± 1.50	1.00 ± 0.03	1.12 ± 0.06	1.17 ± 0.07
Lys2-12	109.96	12.33 ± 1.21	0.47 ± 0.02	1.12 ± 0.06	1.17 ± 0.08
Lys2-21	89.43	11.12 ± 1.57	1.10 ± 0.02	1.10 ± 0.04	1.15 ± 0.07
Lys2-22	97.30	10.20 ± 1.53	0.82 ± 0.02	1.11 ± 0.06	1.17 ± 0.08
Lys2-31	88.49	16.10 ± 2.50	0.56 ± 0.01	1.17 ± 0.22	1.20 ± 0.12
Lys2-32	91.91	14.44 ± 2.53	0.40 ± 0.01	1.16 ± 0.14	1.22 ± 0.10
Lys2-41	102.50	15.13 ± 2.40	0.59 ± 0.02	1.14 ± 0.10	1.17 ± 0.08
Lys2-42	103.08	13.21 ± 1.50	0.42 ± 0.01	1.16 ± 0.16	1.20 ± 0.10
Lys2-C	84.15	14.76 ± 1.63	0.79 ± 0.03	1.15 ± 0.10	1.21 ± 0.10

Table 5

Physical properties and biological activity of C-3-pellets.

Sample	Activity% ( $y_{13}$ )	Hardness(N) ( $y_{23}$ )	MC% ( $y_{33}$ )	Roundness ( $y_{43}$ )	Aspect ratio ( $y_{53}$ )
Lys3-11	79.00	15.23 ± 1.64	0.93 ± 0.03	1.17 ± 0.13	1.18 ± 0.11
Lys3-12	76.47	13.35 ± 2.02	0.55 ± 0.02	1.17 ± 0.10	1.16 ± 0.07
Lys3-21	84.81	15.26 ± 2.10	0.94 ± 0.04	1.17 ± 0.13	1.17 ± 0.10
Lys3-22	74.51	13.28 ± 1.58	0.65 ± 0.02	1.16 ± 0.10	1.17 ± 0.10
Lys3-31	87.18	15.95 ± 2.61	0.67 ± 0.05	1.16 ± 0.08	1.24 ± 0.10
Lys3-32	77.66	14.21 ± 2.26	0.59 ± 0.03	1.20 ± 0.16	1.28 ± 0.14
Lys3-41	92.79	12.83 ± 2.18	0.97 ± 0.03	1.21 ± 0.14	1.22 ± 0.12
Lys3-42	79.17	11.01 ± 1.32	0.72 ± 0.07	1.22 ± 0.11	1.20 ± 0.10
Lys3-C	66.67	13.77 ± 1.48	0.83 ± 0.03	1.24 ± 0.20	1.23 ± 0.10

increment of both impeller speed and liquid addition rate significantly ( $p < 0.05$ ) increased the enzyme activity (Eq. (6)). A further difference is that in the case of C1 the increasing liquid addition rate clearly has a positive effect (coefficients  $b_1$  and  $b_{12}$ ) on enzyme activity by the compensation of the temperature excess caused by higher friction. In

contrast, for C2 the negative value of coefficient  $b_{12}$  indicates the negative effect of a high dosing rate when low shear rates are applied. This supports our previous conclusion [1,22,23] that the over-wetting of the enzyme increases its sensitivity to thermomechanical stress. The higher biological activity of C2 and the considerably lower enzyme

activity of C3 support our argument concerning the impact of the critical material attributes, especially the deformability of particles, on the quality of the macromolecular product. Consequently, the variation in the properties of formulation excipients or a macromolecular drug results in different biological activities and different thermal behaviors in response to the elevated mechanical stress, and the differences in factor coefficients and interactions indicate that it will exert considerable impact on the design space too.

### 3.2.2. Mechanical properties and moisture content

All the prepared pellet samples showed fairly good breaking force (10.20–16.10 N), making them to be qualified for the subsequent coating process, which requires the granules to be hard enough to withstand the mechanical attrition encountered during the coating process.

$$y_{21} = 13.49 + 0.195x_1 - 0.440x_2 - 0.808x_3 + 0.555x_{1x2} + 0.173x_{1x3} + 0.358x_{2x3}$$

$$R^2_{adj} = 0.9654MS \text{ Residual} = 0.0481Curv. \text{ coeff.} = 0.5500 \quad (8)$$

$$y_{22} = 13.19 + 1.528x_1 - 0.778x_2 - 0.648x_3 + 0.228x_{1x2} - 0.248x_{1x3} - 0.063x_{2x3}$$

$$R^2_{adj} = 0.9999MS \text{ Residual} = 0.0001Curv. \text{ coeff.} = 1.568 \quad (9)$$

$$y_{23} = 13.89 - 0.390x_1 - 0.795x_2 - 0.928x_3 - 0.785x_{1x2} + 0.038x_{1x3} - 0.023x_{2x3}$$

$$R^2_{adj} = 0.9999MS \text{ Residual} = 0.0005Curv. \text{ coeff.} = -0.1200 \quad (10)$$

Despite the considerably high values of the coefficients, none of the factors showed statistical significance in the case of C1 (Eq. (8)). In contrast, their effects on C2 and C3 were clearly significant (Eqs. (9) and (10)). Increasing the impeller speed increases the hardness of C1 and C2 while decreasing the breaking force of C3, which indicates that increasing friction has a negative influence on the bonding ability of mechanically resistant particles. An increase in both liquid addition rate ( $x_2$ ) and extrusion speed ( $x_3$ ) decreases hardness in all cases, which may be related to the less uniform distribution of water and particle density, which considerably influences the internal texture of the pellets. The deformation of the pellets starts with a viscoelastic deformation to the increasing load. No visible change in the shape of the pellets may be observed during this stage. In the next phase, plastic deformation of the pellets results in complete crushing of the pellets (Fig. 6). In some cases, a multi-stage deformation process was observed (Fig. 6b), where the first peak indicates the presence of microfractures due to small inconsistencies or structural defects in the pellet texture without visible deformations or breakage of the pellets. Therefore, peak C, which is equal to the crushing strength, was considered as pellet hardness in all cases.

The results revealed that the observed differences in the stability, polymorphs or mechanical properties of the raw materials did not affect the water uptake pattern of the various compositions (0.6 ml/g).

Therefore, the physical interactions upon liquid (water) addition and mixing were almost similar for all formulations (C1–C3) processed under the same experimental conditions and confirmed by the comparable moisture content of the formulations processed under the same conditions. In case of C1 and C2, a weaker model quality was observed, which may be related to the higher values of curvature coefficients of these compositions, which indicates certain nonlinearity of the effect of the factors. Due to the weaker fit, the resulting models should be evaluated with cautions. The most considerable effect was exerted by the extruder speed ( $x_3$ ), but it was found significant only for C1 (Eq. (11)). The results indicate higher extrusion rates may repulse water from the wet mass and so decrease the final MC of the pellets.

$$y_{31} = 0.566 - 0.059x_1 - 0.044x_2 - 0.126x_3 + 0.051x_{1x2} - 0.036x_{1x3}x_3$$

$$R^2_{adj} = 0.8544MS \text{ Residual} = 0.0045Curv. \text{ coeff.} = 0.2038 \quad (11)$$

$$y_{32} = 0.670 - 0.178x_1 + 0.063x_2 - 0.143x_3 - 0.050x_{1x2} + 0.060x_{1x3} - 0.033x_{1x2}x_3$$

$$R^2_{adj} = 0.8899MS \text{ Residual} = 0.0072Curv. \text{ coeff.} = 0.1200 \quad (12)$$

$$y_{33} = 0.753 - 0.015x_1 + 0.068x_2 - 0.125x_3 + 0.040x_{1x2} + 0.043x_{1x3} - 0.033x_{1x2}x_3$$

$$R^2_{adj} = 0.9688MS \text{ Residual} = 0.0008Curv. \text{ coeff.} = 0.0775 \quad (13)$$

According to the literature, Colley et al. reported that increasing the moisture content of pellets is accompanied by increasing their breaking force up to a certain moisture content, and then further moisture will reduce their breaking hardness [30]. However, the increase in the moisture content in a formulation which contains macromolecules is problematic because it reduces the long-term stability and adversely affects biological activity [31]. Generally, the moisture content of all the prepared samples was good (max.1.1 %) and could be maintained by appropriate packaging and storage conditions.

### 3.2.3. Roundness and aspect ratio

The preformulation study showed that the maximum spherization time was 1 min, therefore it was kept constant for all the prepared samples as a result of the incorporation of a higher amount of polyols, which are hygroscopic and have a tendency to develop electrostatic charges, thus increasing the spherization time will lead to the sticking of the pellets [32,33].

The roundness of all the produced samples of C1 and C2 was good ( $<1.2$ ), while C3 showed slightly higher values ( $\leq 1.28$ ). As known, the closer roundness is to 1, the closer the sample shape is to circular, thereby allowing the pellets to be coated effectively. According to the literature, the sphericity of the pellets is markedly affected by the quantity of the granulating liquid and the duration of spherization time [34]. The liquid addition rate had a significant effect on pellet roundness for C1 and C2 (Eqs. (14) and (15)), but significance should be evaluated with caution in case of C1, due to the poorer model quality. Interestingly, the increasing liquid addition rate increased the roundness

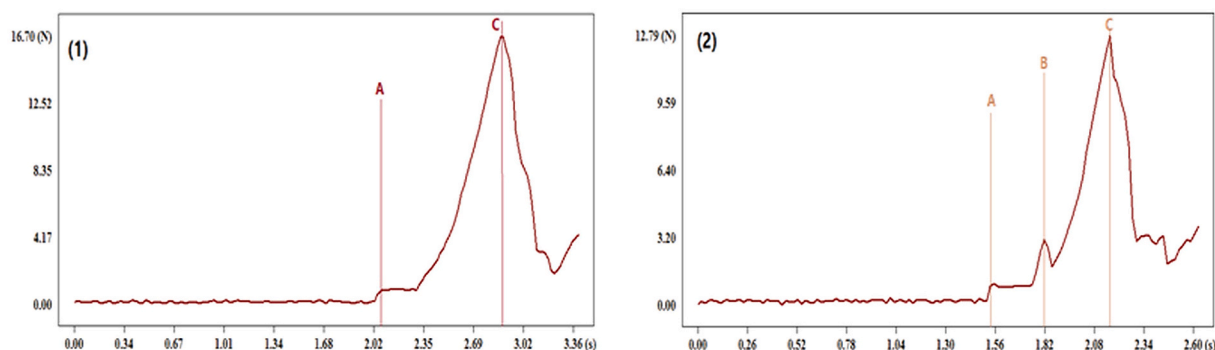


Fig. 6. (1 and 2). Typical pellet deformation curves, A and B: viscoelastic stages of deformation and C the final collapse of the pellet.

of C1 and C3 while decreasing the roundness of C2. This could be attributed to the different material characteristics, especially to the different deformation characteristics of SDM. The fact that the impeller speed affected roundness significantly only for C2 and the significance of the curvature coefficient of the same composition indicate that the uniformity of liquid distribution had a significant impact on the sphericity of C2. Impeller speed also had a significant effect on the AR of C2 and C3 (Eqs. (18) and (19)), it was directly proportional to AR and the interaction of the tested factors was not significant.

$$y_{41} = 1.143 + 0.010x_2 - 0.005x_3 - 0.010x_1x_2 + 0.005x_1x_3 \quad (14)$$

$$R^2_{adj} = 0.8252MS \text{ Residual} = 0.00005\text{Curv. coeff.} = -0.013$$

$$y_{42} = 1.135 + 0.023x_1 - 0.008x_2 + 0.005x_2x_3 + 0.003x_1x_2x_3 \quad (15)$$

$$R^2_{adj} = 0.9733MS \text{ Residual} = 0.00002\text{Curv. coeff.} = 0.015$$

$$y_{43} = 1.183 + 0.015x_1 + 0.005x_2 + 0.005x_3 + 0.010x_1x_2 + 0.008x_1x_3 - 0.005x_2x_3 \quad (16)$$

$$R^2_{adj} = 0.9419MS \text{ Residual} = 0.00005\text{Curv. coeff.} = 0.058$$

$$y_{51} = 1.15 + 0.005x_2 - 0.005x_3 - 0.013x_1x_2 + 0.003x_1x_3 + 0.003x_1x_2x_3 \quad (17)$$

$$R^2_{adj} = 0.9072MS \text{ Residual} = 0.00003\text{Curv. coeff.} = -0.0200$$

$$y_{52} = 1.181 + 0.016x_1 - 0.009x_2 + 0.009x_3 - 0.004x_1x_2 + 0.004x_1x_3 + 0.004x_2x_3 \quad (18)$$

$$R^2_{adj} = 0.9774MS \text{ Residual} = 0.00001\text{Curv. coeff.} = 0.0275$$

$$y_{53} = 1.203 + 0.033x_1 - 0.013x_2 - 0.013x_1x_2 - 0.005x_2x_3 - 0.001x_1x_2x_3 \quad (19)$$

$$R^2_{adj} = 0.9376MS \text{ Residual} = 0.0001\text{Curv. coeff.} = 0.0275$$

### 3.3. Evaluation of the changes on the process design space

It is clear from the results of the previous chapter (3.2) that the different compositions showed considerable differences in the response to changes in process parameters, which greatly influenced the size and position of the process design space (DS) in the modeled knowledge space. The DS was determined according to the recommendations of Appendix 2 of the ICH Q8 guideline, using the following acceptance

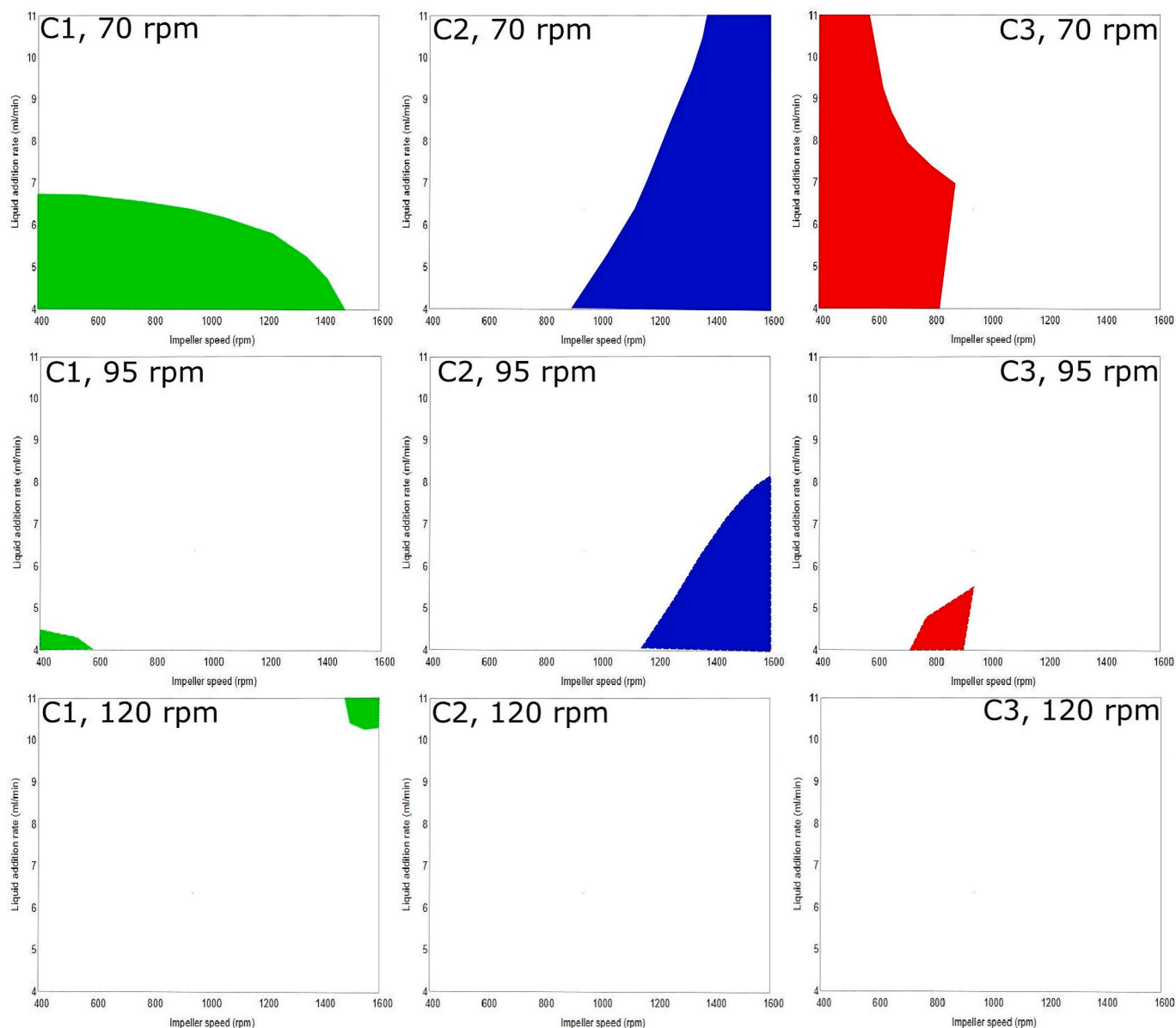


Fig. 7. Design space of the kneading process in case of various compositions and extruder speeds.

criteria in case of various CQAs: enzyme activity >75 %, pellet hardness >15 N, moisture content <1 %, aspect ratio <1.2, roundness <1.2. The contour plots of CQAs (Figs. S5–S49) and the scheme of the determination of the DS (Fig. S50) can be found in the supplementary material, while Fig. 7 shows the position of DS of different compositions at different extruder speeds.

The results showed that the enzymatic activity and the moisture content were the less limiting factors, and the DS were mostly determined by the overlapping portions of the acceptance areas of hardness and shape parameters. Since increasing of the extruder speed generally reduced the hardness and worsened shape parameters, this resulted in a decrease in the size of the DS of all compositions. The results showed that DS only partially overlap in case of the different formulations. A liquid feed rate of 4–5 ml/min and an impeller speed of 1100–1300 rpm and an extruder speed of 70 rpm can be used as controls for samples C1 and C2, while for sample C3 a liquid feed rate of 4–5 ml/min and 750–800 rpm min impeller speed can be used at an extruder speed of 70–95 rpm.

#### 4. Conclusion

The specially designed granulation chamber equipped with seven sensors was a useful tool to precisely monitor the changes in the temperature and RH% during the course of high shear kneading. Therefore, the chamber could be used effectively to produce proteins/peptides and other thermolabile drugs, and to correlate the processing conditions with the product quality of these drugs. The continuous monitoring of the changes in temperature and RH% enables the precise determination of the critical points of differently set processes and hence could be used as a novel tool for both process analytical technology (PAT) and QbD.

This has a particular importance in case of strongly thermolabile drugs such as lysozyme. Nevertheless, despite the predominant concept according to which most technologist researchers think that the effect of mechanical attrition and elevated temperature on the processed macromolecules will end in an inactive product as a result of protein folding or deterioration, present work confirmed that lysozyme could be processed under high-shear conditions. Furthermore, we were able to prove our hypothesis that with careful design, enzyme activity can be maintained as desired even when working with less stable forms of enzyme, such as lyso-2.

It could also be concluded that the investigation of the critical material attributes is essential not only for APIs but also for excipients during the development stage of macromolecular drugs, since they have a major impact on the process temperature, and therefore on biological activity, and other product properties, which became clearer when the mechanical energy input increased. Consequently, the evaluation of the omitted design space is crucial from the aspect of the properties of the formulated materials before the large-scale production of biopharmaceuticals.

#### CRedit authorship contribution statement

**Yousif H-E.Y. Ibrahim:** Investigation, Formal analysis, Writing – original draft. **Patience Wobuoma:** Investigation. **Katalin Kristó:** Formal analysis, Writing – review & editing. **Ferenc Lajkó:** Software, Resources. **Gábor Klivényi:** Software, Resources. **Béla Jancsik:** Software, Resources. **Géza Regdon jr:** Writing – review & editing. **Klára Pintye-Hódi:** Conceptualization, Writing – review & editing. **Tamás Sovány:** Conceptualization, Methodology, Writing – review & editing.

#### Declaration of competing interest

The authors declare that they have no known competing financial interests or personal relationships that could have appeared to influence the work reported in this paper.

#### Acknowledgements

This research was supported by the EU-funded Hungarian grant EFOP-3.6.1-16-2016-00008. The publication was supported by the University of Szeged Open Access Fund Grant No. 5380.

#### Appendix A. Supplementary data

Supplementary data to this article can be found online at <https://doi.org/10.1016/j.jddst.2021.102714>.

#### References

- [1] T. Sovány, Z. Tislér, K. Kristó, A. Kelemen, G. Regdon, Estimation of design space for an extrusion–spheronization process using response surface methodology and artificial neural network modelling, *Eur. J. Pharm. Biopharm.* 106 (2016) 79–87, <https://doi.org/10.1016/j.ejpb.2016.05.009>.
- [2] D.J. Brayden, M.-J. Alonso, Oral delivery of peptides: opportunities and issues for translation, *Adv. Drug Deliv. Rev.* 106 (2016) 193–195, <https://doi.org/10.1016/j.addr.2016.10.005>.
- [3] K. Fuhrmann, G. Fuhrmann, Recent advances in oral delivery of macromolecular drugs and benefits of polymer conjugation, *Curr. Opin. Colloid Interface Sci.* 31 (2017) 67–74, <https://doi.org/10.1016/j.cocis.2017.07.002>.
- [4] V. Truong-Le, P.M. Lovalenti, A.M. Abdul-Fattah, Stabilization challenges and formulation strategies associated with oral biologic drug delivery systems, *Adv. Drug Deliv. Rev.* 93 (2015) 95–108, <https://doi.org/10.1016/j.addr.2015.08.001>.
- [5] M. Bilej, *Mucosal immunity in invertebrates*, in: *Mucosal Immunol*, Elsevier, 2015, pp. 135–144.
- [6] V.L. Hughey, E.A. Johnson, Antimicrobial activity of lysozyme against bacteria involved in food spoilage and food-borne disease, *Appl. Environ. Microbiol.* 53 (1987) 2165–2170.
- [7] K. Düring, P. Porsch, A. Mahn, O. Brinkmann, W. Gieffers, The non-enzymatic microbicidal activity of lysozymes, *FEBS Lett.* 449 (1999) 93–100, [https://doi.org/10.1016/S0014-5793\(99\)00405-6](https://doi.org/10.1016/S0014-5793(99)00405-6).
- [8] S. Nakamura, A. Kato, K. Kobayashi, New antimicrobial characteristics of lysozyme-dextran conjugate, *J. Agric. Food Chem.* 39 (1991) 647–650.
- [9] T. Yada, K. Muto, T. Azuma, K. Ikuta, Effects of prolactin and growth hormone on plasma levels of lysozyme and ceruloplasmin in rainbow trout, *Comp. Biochem. Physiol. C Toxicol. Pharmacol.* 139 (2004) 57–63, <https://doi.org/10.1016/j.cca.2004.09.003>.
- [10] G.G. Syngai, G. Ahmed, Lysozyme: a natural antimicrobial enzyme of interest in food applications, in: *Enzym. Food Biotechnol.*, Elsevier, 2019, pp. 169–179, <https://doi.org/10.1016/B978-0-12-813280-7.00011-6>.
- [11] S. Bhaskaran, P.K. Lakshmi, Extrusion spheronization—a review, *Int J Pharm Tech Res 2* (2010) 2429–2433.
- [12] S. Muley, T. Nandgude, S. Poddar, Extrusion–spheronization a promising pelletization technique: in-depth review, *Asian J. Pharm. Sci.* 11 (2016) 684–699, <https://doi.org/10.1016/j.ajps.2016.08.001>.
- [13] N.R. Trivedi, M.G. Rajan, J.R. Johnson, A.J. Shukla, Pharmaceutical approaches to preparing pelletized dosage forms using the extrusion-spheronization process, *Crit. Rev. Ther. Drug Carrier Syst.* 24 (2007) 1–40, <https://doi.org/10.1615/critrevtherdrugcarriersyst.v24.i1.10>.
- [14] É. Bölcskei, G. Regdon, T. Sovány, P. Kleinebudde, K. Pintye-Hódi, Optimization of preparation of matrix pellets containing Eudragit® NE 30D, *Chem. Eng. Res. Des.* 90 (2012) 651–657, <https://doi.org/10.1016/j.cherd.2011.09.005>.
- [15] M. Hirjau, A.C. Nicoara, V. Hirjau, D. Lupuleasa, Pelletization techniques used in pharmaceutical fields, *Farma 4* (2011) 4.
- [16] L. Palugan, M. Cerea, L. Zema, A. Gazzaniga, A. Maroni, Coated pellets for oral colon delivery, *J. Drug Deliv. Sci. Technol.* 25 (2015) 1–15, <https://doi.org/10.1016/j.jddst.2014.12.003>.
- [17] D.F. Erkoboni, Extrusion-spheronization as a granulation technique, *Drugs Pharmaceut. Sci.* 81 (1997) 333–368.
- [18] R. Gandhi, C. Lal Kaul, R. Panchagnula, Extrusion and spheronization in the development of oral controlled-release dosage forms, *Pharmaceut. Sci. Technol. Today 2* (1999) 160–170, [https://doi.org/10.1016/S1461-5347\(99\)00136-4](https://doi.org/10.1016/S1461-5347(99)00136-4).
- [19] C.L.S. Lau, Q. Yu, V.Y. Lister, S.L. Rough, D.I. Wilson, M. Zhang, The evolution of pellet size and shape during spheronisation of an extruded microcrystalline cellulose paste, *Chem. Eng. Res. Des.* 92 (2014) 2413–2424.
- [20] H. Rezaei, C.J. Lim, A. Lau, S. Sokhansanj, Size, shape and flow characterization of ground wood chip and ground wood pellet particles, *Powder Technol.* 301 (2016) 737–746, <https://doi.org/10.1016/j.powtec.2016.07.016>.
- [21] M. Eriksson, G. Alderborn, C. Nyström, F. Podczek, J.M. Newton, Comparison between and evaluation of some methods for the assessment of the sphericity of pellets, *Int. J. Pharm.* 148 (1997) 149–154.
- [22] T. Sovány, K. Csordás, A. Kelemen, G. Regdon, K. Pintye-Hódi, Development of pellets for oral lysozyme delivery by using a quality by design approach, *Chem. Eng. Res. Des.* 106 (2016) 92–100, <https://doi.org/10.1016/j.cherd.2015.11.022>.
- [23] K. Kristó, O. Kovács, A. Kelemen, F. Lajkó, G. Klivényi, B. Jancsik, K. Pintye-Hódi, G. Regdon, Process analytical technology (PAT) approach to the formulation of thermosensitive protein-loaded pellets: multi-point monitoring of temperature in a high-shear pelletization, *Eur. J. Pharmaceut. Sci.* 95 (2016) 62–71, <https://doi.org/10.1016/j.ejps.2016.08.051>.

- [24] S.A. Abbas, V.K. Sharma, T.W. Patapoff, D.S. Kalonia, Opposite effects of polyols on antibody aggregation: thermal versus mechanical stresses, *Pharm. Res. (N. Y.)* 29 (2012) 683–694, <https://doi.org/10.1007/s11095-011-0593-4>.
- [25] S. Singh, J. Singh, Effect of polyols on the conformational stability and biological activity of a model protein lysozyme, *AAPS PharmSciTech* 4 (2003) 101–109.
- [26] Q.-B. Ding, P. Ainsworth, G. Tucker, H. Marson, The effect of extrusion conditions on the physicochemical properties and sensory characteristics of rice-based expanded snacks, *J. Food Eng.* 66 (2005) 283–289, <https://doi.org/10.1016/j.jfoodeng.2004.03.019>.
- [27] J.A.C. Elbers, H.W. Bakkenes, J.G. Fokkens, Effect of amount and composition of granulation liquid on mixing, extrusion and spheronization, *Drug Dev. Ind. Pharm.* 18 (1992) 501–517, <https://doi.org/10.3109/03639049209043708>.
- [28] T. Schæfer, C. Mathiesen, Melt pelletization in a high shear mixer. VIII. Effects of binder viscosity, *Int. J. Pharm.* 139 (1996) 125–138, [https://doi.org/10.1016/0378-5173\(96\)04549-8](https://doi.org/10.1016/0378-5173(96)04549-8).
- [29] W.L. Hulse, R.T. Forbes, M.C. Bonner, M. Getrost, The characterization and comparison of spray-dried mannitol samples, *Drug Dev. Ind. Pharm.* 35 (2009) 712–718, <https://doi.org/10.1080/03639040802516491>.
- [30] Z. Colley, O.O. Fasina, D. Bransby, Y.Y. Lee, Moisture effect on the physical characteristics of switchgrass pellets, *Trans. ASABE (Am. Soc. Agric. Biol. Eng.)* 49 (2006) 1845–1851, <https://doi.org/10.13031/2013.22271>.
- [31] Y.-F. Maa, P.-A. Nguyen, J.D. Andya, N. Dasovich, T.D. Sweeney, S.J. Shire, C. C. Hsu, Effect of spray drying and subsequent processing conditions on residual moisture content and physical/biochemical stability of protein inhalation powders, *Pharm. Res. (N. Y.)* 15 (1998) 768–775.
- [32] L. Gu, C.V. Liew, P.W.S. Heng, Wet spheronization by rotary processing—a multistage single-pot process for producing spheroids, *Drug Dev. Ind. Pharm.* 30 (2004) 111–123, <https://doi.org/10.1081/DDC-120028706>.
- [33] C. Vecchio, G. Bruni, A. Gazzaniga, Research papers: preparation of indobufen pellets by using centrifugal rotary fluidized bed equipment without starting seeds, *Drug Dev. Ind. Pharm.* 20 (1994) 1943–1956, <https://doi.org/10.3109/03639049409049329>.
- [34] K. Lövgren, P.J. Lundberg, Determination of sphericity of pellets prepared by extrusion/spheronization and the impact of some process parameters, *Drug Dev. Ind. Pharm.* 15 (1989) 2375–2392.